ORGANISATION EUROPEENNE POUR LA RECHERCHE NUCLEAIRE
EUROPEAN ORGANIZATION FOR NUCLEAR RESEARCH

Laboratoire Européen pour la Physique des Particules
European Laboratory for Particle Physics

CERN-PH-EP/2006-025
21 August 2006

The X-HPD – Conceptual Study of a Large Spherical Hybrid Photodetector

A.Braem[a], C.Joram[a,*], J.Séguinot[a], P. Lavoute[b], C. Moussant[b]

[a] *CERN, PH Department, CH-1211 Geneva, Switzerland*

[b] *Photonis SAS, F-19100 Brive La Gaillarde, France*

Abstract

We present the results of a conceptual study demonstrating the feasibility of a large spherical hybrid photodetector with central anode. A prototype tube with 208 mm diameter and an anode in form of a metallic cube has been fabricated. In the final version of the so-called X-HPD concept the anode will be a scintillator cube with plated faces and a small photodetector to read out the bottom. The bialkali photocathode covers three quarters of the sphere surface. Combined use of this cathode in transmissive and reflective mode leads to effective quantum efficiency values exceeding those obtained in conventional hemispherical PMT designs. Further features of the concept are a photoelectron collection efficiency approaching 100% and a photon amplification in the scintillator crystal leading to a distinct single photoelectron signal.

Using a custom built electron accelerator based on a CsI transmissive photocathode, LSO and YAP block crystals in geometries adapted to the anode of an X-HPD have been tested with single photoelectrons in the 10-30 keV energy range. The scintillation light was read out with a conventional PMT or a Si-PM. More than 30 photoelectrons per incident electron could be detected with the PMT.

Submitted to Elsevier

Keywords: Photodetector, HPD, scintillator, Si-PM
PACS 85.60.Ha, 85.60.Dw, 29.40.Ka, 95.55.Vj

* Corresponding author: Christian.Joram@cern.ch

1. Introduction

The instrumentation of a water volume with photodetectors allows building neutrino telescopes in the kton to Mton range, be it in form of a water tank in a deep underground cavern or in natural aqueous media like sea water or ice. Photosensors are used to detect Cherenkov light emitted by fast secondary charged particles which originate from neutrino interactions. Past and current experiments relied on hemispherical photomultiplier tubes, typically of 8 – 20" diameter, which are protected in robust glass spheres from the hydrostatic pressure in case they need to be deployed in the deep sea or ice.

Conceptual studies and R&D activities (e.g. C2GT [1], KM3net [2] MEMPHYS, Hyper-Kamiokande [3]) for the next generation of neutrino telescopes are looking for cost-effective ways to instrument ever increasing volumes with tens to hundreds of thousands of photodetectors. A recent overview article on Cherenkov instrumentation in astroparticle physics can be found in [4].

Key parameters to be optimized are effective quantum efficiency (QE × photoelectron collection efficiency) and active area. High gain allows for the use of simpler and potentially cheaper electronics. Low transit time spread (TTS) is needed to reconstruct the wave front of the Cherenkov cone. Simplicity, i.e. a low number of relatively cheap components, and highly automated fabrication are necessary ingredients for cost-effectiveness. Robustness and reliability are absolute musts if maintenance-free operation over long periods of time is required.

The development presented in this article aims at meeting the above goals with the X-HPD[1] concept (section 2). Originally started in the framework of the C2GT study [5] the X-HPD has become a more general photodetector R&D project.

2. The X-HPD concept

The X-HPD (see Fig. 1) consists of a practically spherical glass envelope on which a semitransparent photocathode is evaporated and a cubic or spherical anode for the detection of the photoelectrons in the centre of the sphere.

The central location of the anode brings about three main advantages: (1) the anode can detect photoelectrons in a large solid angle range (~3π), (2) all photoelectrons have practically the same pathlength (the transit time spread is well below 1 ns), and (3) the photoelectron collection efficiency reaches values close to 100%.

The fact that the photocathode covers more than ¾ of the sphere surface leads to a further welcome phenomenon. Light which is not absorbed by the semitransparent photocathode has a second chance to be detected on the opposite side of the sphere, then in reflective mode. For the same thickness the QE in reflective cathode is generally higher than in semitransparent mode. Consequently the effective quantum efficiency of the X-HPD can be significantly larger than for a conventional PMT design. The price to pay is a contribution of about 1 ns to the transit time for the fraction of the light which is converted only at the second occasion.

In our original design [5] the anode consisted of a ceramic cube (1.5 cm side length) of which 4 sides and the upper face were covered with silicon sensors of 1.5 × 1.5 cm^2 area. The gain mechanism is based on the conversion of the kinetic energy of the photoelectron in electron hole pairs in the depleted Si sensor ($W_{e\text{-}h}$ = 3.6 eV). The charge gain is of the order of $5 \cdot 10^3$ for a voltage of 20 kV. The smallness of the signal calls for segmented Si sensors with lower capacitance (few pF) to reduce the intrinsic electronics noise and so to improve the signal-to-noise ratio.

Inspired by earlier developments like the Philips Smart tube concept [6] and the Lake Baikal Quasar tube [7] as well as by the availability of modern high performance inorganic scintillators we varied or design by replacing the Si-sensor with a scintillator block crystal. Crystals like YAP:Ce and LSO:Ce achieve light yields of 15-20

[1] The name 'X-HPD' alludes to the use of a scintillator crystal (= Xtal) as amplifying structure. The 'X' symbolizes also the trajectories coming radially from all directions and hitting the crystal in the centre of the HPD.

photons per keV deposited energy, have short decay times (~25 ns) and are compatible with the required bakeout cycles of a photocathode process.

The X-HPD is actually concentrating and multiplying the photons. In contrast to conventional PMTs it truly deserves the name 'photomultiplier'. Five sides of the crystal are coated with a thin (~100 nm) reflective Al layer, the sixth lower side is interfaced to a photomultiplier. In past devices inexpensive PMTs of small diameter were employed for this purpose. Again, recent progress in the field of Geiger mode APDs [8] [9] (also referred to as Si-PMs) provide the option of replacing the PMT by a miniature and potentially cheaper solid state device which could beat the PMT in terms of QE. Currently the size of existing GM-APDs is still limited to sizes of up to 3 x 3mm^2 and their QE in the blue part of the spectrum (~10%) remains well below the one of a good PMT (25-30 %). Also their dark count rates at the single photoelectron level (~ MHz/mm^2 at 20°C) lies 5 orders of magnitude above the one of a bialkali photocathode (~ 10 Hz/mm^2).

Of the typically 300 scintillation photons generated by a 20 keV photoelectron in a crystal of 1 cm^3 volume only about one third arrive at the photodetector. The rest is absorbed in the bulk or in wall reflections. Depending on surface coverage and quantum efficiency the gain of this pre-amplification stage is of the order 5 – 30.

3. Fabrication and test of a prototype with metal anode

We fabricated a prototype tube of 208 mm external diameter (see Fig. 2) with a cubic metal anode of 1 cm^3 volume. The cube is supported in the centre of the spherical envelope by a ceramic tube fixed on the base plate of the tube. More details about the tube design can be found in [5] and [10].

The semitransparent bialkali (K_2CsSb) photocathode was evaporated in our transfer facility at CERN [11]. The tube is in-situ sealed with the stainless steal base plate of 127 mm diameter. Two Al ring electrodes are evaporated in a preparatory step. The upper electrode serves as contact to the photocathode. The lower one is used to correct for field distortions in the non-spherical lower part of the tube. Our transfer process avoids any alkali metal deposits on the anode and its support. This is the region with the highest E-field and hence the highest probability of electrical discharges. A cylindrical evaporation mask limits the photocathode deposition to the hemisphere above the upper electrode.

3.1. QE measurements

The 208 mm tube was too large to fit in our standard QE test set-up at CERN. QE was online-monitored during the cathode evaporation for process optimisation. However under these conditions[2] the strength and the geometry of the electric field were far from optimal and the measured QE served only for the optimization of the cathode performance.

The QE for top and side illumination was therefore measured in the standard set-up at Photonis[3] using a collimated white light source with a set of interference filters. The diameter of the light spot was about 44 mm. The photocurrent emitted from the cathode was measured while the applied voltage at the anode was varied between +500 and +1000 V. At the latter voltage the photocurrent appeared to be practically saturated. QE was calculated by relating the measured photocurrent for each wavelength to the ones measured with a certified calibrated PMT. The results of the two measurements (side and top illumination) are shown in Fig. 3. For top illumination the light can only be converted by the cathode in semitransparent mode. For side illumination the incident light had a double chance of being converted. The ratio QE_{side} / QE_{top} was about 2.1 (see dashed line in Fig. 3), practically independent of the wavelength. The large value of the ratio confirmed the subjective impression that the cathode is relatively thin, which was also supported by its somewhat weak red-response.

---

[2] A cylindrical mask around the evaporation sources can be set to a maximal voltage of +500 V and serves as anode.

[3] PHOTONIS SAS, Brive, France

3.2. Uniformity of sensitivity

Azimuthal and polar scans over the surface of the prototype detector were performed in a dark box at CERN using a blue LED (Bivar LED3-UV-400-30, λ = 400 nm, ±15° emission angle) which was manually displaced and oriented normal to the cathode surface. The anode was set to +300V, cathode and corrector electrode were maintained at ground potential. The measured photocurrents emitted from the cathode were normalized to the highest value obtained in one scan (θ or ϕ). The azimuthal scan was performed in the equatorial plane, i.e. at θ = 90°. The results are shown in Fig. 4. The polar scan shows an expressed angular dependence with minimum (maximum) sensitivity at θ = 90° (0°). Taking into account the divergence of the LED source which dilutes the distribution the peak-to-valley ratio of 1.7 is in reasonable agreement the factor ~2 difference between top and side illumination measured at Photonis. The azimuthal scan reveals full symmetry as expected for this design.

3.3. High voltage tests

The prototype tube has been operated in air at cathode voltages up to -20 kV without significant leakage currents (< nA). The tube was powered in a kapton lined tank up to -30 kV however the used power supply allowed only to derive an upper limit for the leakage current of 0.2 μA. No signs of discharges were observed. The opposite powering, i.e. anode at +HV and cathode at ground could not be tested above 1000 V, as the anode is supplied by a simple vacuum feedthrough in the base plate which is not HV rated.

4. Characterization of scintillation crystals for the X-HPD

The suitability of a scintillation crystal as anode in the X-HPD depends on a number of properties: light yield, peak wavelength of emission, decay time, mechanical and thermal stability, machinability, price and availability. While in in the Quasar tube a YSO (Y_2SiO_5:Ce) scintillator disk and in the Philips Smart tube a P47 phosphor disk were used we propose scintillators with block shape in order to exploit a larger solid angle. A broad range of high performance inorganic crystals has been developed over the last decade which is now finding applications mainly in medical imaging (e.g. PET, SPECT). Among those the Ce^{3+} doped crystals YAP, LSO, LYSO, LuAP and LuAG [12] are particularly interesting for our application. They combine high light yield (~20-30 ph/keV) with short decay time (18-70 ns) and have an emission spectrum around peaked around 400 nm, except for LuAg which peaks at 535 nm. The new La based crystals $LaBr_3$ and $LaCl_3$ have even higher light yield (40 – 60 ph/keV) and shorter decay time however they are hygroscopic which makes their handling difficult.

To test the X-HPD concept we have prepared a YAP ($YAlO_3$) and a LSO (Lu_2SiO_5) crystal of 10 × 10 × 10 mm^3 size. Five sides were coated with a 100 nm thick Al layer which was evaporated in vacuum. The sixth side which faces the photodetector was left uncoated. While the LSO crystal was provided by the manufacturer optically polished, we used a circular saw with diamond disk to cut the YAP crystal from a larger block[4] of Russian origin and polished it to optical quality. The optical absorption length of both crystals was measured with a spectrophotometer: λ_{abs}(LSO) = 210 mm, λ_{abs}(YAP) = 100 mm.

A Monte-Carlo photon tracking code was used to estimate the number of photons hitting the cathode of the photosensor. The program which was written by one of the authors (C.J.) takes into account bulk absorption, surface reflections, refraction and total internal reflection at the interfaces. In the case of LSO, based on a light yield of 26.000 photons / MeV[5] and a reduced relative light yield at low electron energies [13] [14], e.g. 77.6% at 20 keV, an electron of 20 keV energy would produce 390 scintillation photons (at λ = 420 nm). This takes into account a small energy loss (<0.5 keV) in the reflective Al layer. With a measured optical absorption length of 210 mm, the number of photons hitting the photocathode was found to range from 118 (reflectivity of the Al

[4] The block originates from the Russian Research Institute for the Synthesis of Minerals, Alexandrov, Russia.
[5] The light yield of LSO and YAP were taken from material data sheets provided by Saint-Gobain Crystals, 77794 Nemours, France

layer R_{Al} = 0.8) to 135 (R_{Al} = 0.9). Quantum efficiency values in the 20% range would consequently lead to 13 – 27 detected photons. The light yield of YAP is only about 18.000 photons / MeV and our crystal had only an absorption length of 100 mm, however the relative light yield of YAP is 100% also at low energies. The simulation predicts photoelectric yields which remain about 15% below the ones of LSO.

If, instead of covering the full crystal surface, a smaller photosensor (e.g. Si-PM) was used which covered only part of the surface, e.g. 3 × 3 mm^2, the number of photons hitting the sensor would decrease to about 28 (LSO). It was assumed that the part of the bottom surface which was not covered by the photosensor was also Al-coated.

4.1. Experimental set-up

A small pumped vacuum set-up was built which allows exposing the crystal under test to photoelectrons from a semitransparent CsI photocathode (see Fig. 5). The photoelectrons were released from the cathode by light pulses from a self-triggering H_2 flash lamp which emits a VUV spectrum peaked at round 160 nm. The pick-up signal of the lamp was used to generate a trigger for the readout. The intensity of the flash lamp could be controlled by a set of mesh filters. Unless explicitly mentioned the intensity was reduced to single photon level. The photoelectrons were then accelerated by a potential difference of up to 30 kV and deposit their kinetic energy in the scintillator crystal. The scintillation light was viewed through a 1 mm thick sapphire window by a photosensor outside the vacuum tank. Optical grease was used on both sides of the window to improve the optical coupling. As photosensor we used a Photonis XP3102 PMT with bialkali photocathode. Alternatively a blue sensitive Si-PM (type AMPD MW-3[6]) of 3 × 3 mm^2 size was tested. The signals were recorded with a digital oscilloscope (LeCroy Wavemaster LT344, analogue bandwidth 500 MHz) which also allowed histogramming the data.

4.2. Results

4.2.1. PMT readout

Typical waveforms which were obtained by reading the LSO crystal with the PMT are shown in Fig. 6. The exponential decay of the scintillation light is clearly visible. Exponential fits reveal decay constants which are compatible with LSO characteristics. The digital scope was used to integrate the waveform which leads to signals which were proportional to the charge amplitude. These were then histogrammed and fitted. Examples of such charge histograms are shown in Fig. 7 where the voltage at the CsI cathode was varied between 15 and 25 kV. The signal (1 p.e. peak) is clearly separated from the pedestal. The separation increases with the applied HV. The continuum between the pedestal and the 1 p.e. peak is attributed the backscattering of the photoelectron from the LSO crystal ($<Z_{LSO}>$=24.5, back scattering coefficient $\eta \sim 25\%$ [15]). A pedestal cut will discard only a small fraction of the back scattered electrons such that the detection efficiency is expected to remain close to 100%.

The fit function consisted of Gaussians for the pedestal and the 1 p.e. peak plus an exponential describing the backscattering continuum. From analysing the width σ and position μ of the 1 p.e. distribution the number of photoelectrons detected by the PMT can be derived from eq. 1

$$N_{p.e.} = ENF \cdot \frac{\mu^2}{\sigma^2} \tag{1}$$

[6] This particular type of Si-PM, called Avalanche Microchannel Photodiode (AMPD), was produced by the Joint Institute of Nuclear Research in collaboration with the company Mikron (Zelenograd, Russia).

with *ENF* being the excess noise factor of the PMT. In the absence of specific data for the used PMT we chose the value of *ENF* = 1.4 generally quoted in literature. The results of this analysis are plotted in Fig. 8 as a function of the applied acceleration voltage *U*. The fits follow the form

$$N_{p.e.} = A \cdot U \cdot RLO(E) \tag{2}$$

where *RLO(E)* is the energy dependent Relative Light Output, which in case of LSO is taken from [13] [14] and in case of YAP is 100%. The parameter *A* is a free overall normalization determined by the fit. The data are well described by this parameterization. A single photoelectron bombarding the LSO (YAP) crystal at 25 keV energy leads to 34 (24) detected p.e.'s in the PMT.

Fig. 9 shows a charge spectrum which was taken with LSO at 30 kV and with a higher intensity of the flash lamp. The peaks of the second and third photoelectrons as well as the onset of the fourth are visible.

4.2.2. Si-PM readout

The 3 × 3 mm^2 Si-PM was tested in a dedicated test set-up at CERN. The following characteristics were found: effective quantum efficiency at 420 nm = 12%, gain at 130 V = 60.000, dark noise count rate at T = 23°C ≥ 30 MHz, equivalent noise charge (ENC) during a 55 ns gate ~ 2.5 photoelectrons.

From the estimated number of photons (~20) hitting a 3×3 mm^2 sensor from the LSO crystal it was obvious that only a very low photoelectric yield (~2) could be expected. Reading out the YAP crystal (λ = 380 nm) was not tried because the *QE* at this wavelength is below 5%.

Under regular conditions (ambient temperature) the detection of such a low signal proved impossible with the available Si-PM. No signal from the LSO crystal could be detected exceeding the dark noise level.

5. Conclusions and outlook

The results presented in sections 3 and 4 demonstrate the great potential of the X-HPD concept for the instrumentation of large volume water based neutrino telescopes. The spherical geometry leads to a viewing angle of ±120° (or an active solid angle of 3π) combined with a *QE* enhancement due to the *de facto* combination of a semitransparent and a reflective cathode. Over a large part of the detector surface peak QE in excess of 40% can be expected. Detailed characterization of collection efficiency and angular dependence as well as studies of timing properties remain to be done once the X-HPD concept is implemented with a scintillator crystal as anode.

The currently available blue sensitive Si-PM technology appears not yet to achieve the performance required for our application. The excessive dark count rate is the main obstacle when very low light levels are to be detected, however also improvement of gain and quantum efficiency is desirable.

We conclude that PMT readout of the scintillator crystal is currently the preferred solution. The observed photoelectric yield of about 30 promises full detection efficiency, a well defined single photoelectron signal and even modest photon counting capability.

The development of a sealed X-HPD with crystal anode and PMT readout is under way in close collaboration with the company Photonis.

Acknowledgements

We would like to thank our technical staff C. David and M. van Stenis, (both CERN) for their excellent work in the preparation of the mechanical, optical and electronic detector components. The advice and technical support by the Photonis technical team and the continuous support by C. Fontaine was highly appreciated. We would like to thank C.L. Melcher (CPS Innovations) and D. Renker (PSI) for providing us with LSO and YAP block crystals. We are very grateful to Y. Musienko (North-eastern University, Boston, USA, and CERN) for characterizing a Si-PM provided by D. Renker. Valuable comments and suggestions by G. Hallewell (CPPM Marseille) were greatly appreciated.

References

[1] A.E. Ball et al., C2GT, Memorandum, CERN-SPSC-2004-025, SPSC-M-723

[2] KM3NeT; a collaboration of 37 institutes from 8 European nations undertaking a 3 year design study for a km3-scale underwater neutrino telescope and a platform for undersea sciences in the Mediterranean sea. http://www.km3net.org

[3] K. Nakamura et al., Int. J. Mod. Phys. **A** 18 (2003) 4053

[4] G. Hallewell, *The status of Cherenkov detectors in astroparticle physics*, Nucl. Instr. Meth. A 553 (2005) 242-255

[5] A.E. Ball et al., *A large spherical HPD for a novel deep-sea neutrino experiment*, Nucl. Instr. Meth. **A** 553 (2005) 85-90.

[6] Bosetti, P.C., et al for the DUMAND collaboration, *An Optical Sensor for DUMAND II* - European Version; Proceedings of the 23rd International Cosmic Ray Conference, Calgary, July 1993. See http://www.phys.hawaii.edu/~dumand/external_reports.html

[7] R. Bagduev et al., Nucl. Instr. Meth. **A** 420 (1999) 138.

[8] Y. Musienko, *Advances in Avalanche Photodiodes*, Proc. of the 42nd Eloisatron workshop, World Scientific (2004) 427-441

[9] D. Renker, *Geiger-mode avalanche photodiodes, history, properties and problems*, Proceedings of the 4th International Conference on New Developments in Photodetection, Beaune 2005, Nucl. Instr. Meth. **A** (2006), in press.

[10] A. Braem et al. , *Development of HPDs for applications in physics and medical imaging*, Nucl. Instr. Meth. **A** (2006), Proceedings of the 4th International Conference on New Developments in Photodetection, Beaune 2005, in press.

[11] A. Braem, C.Joram, F.Piuz, E.Schyns and J.Seguinot, *Technology of photocathode production*, Nucl. Instr. and Meth. **A** 502 (2003) 205.

[12] P. Dorenbos, Light output and energy resolution of Ce3+-doped scintillators, Nucl. Instr. Meth. **A** 486 (2002) 208-213

[13] W. Mengesha et al., IEEE Trans. Nucl. Sci. Vol. 45, No. 3 (1998) 456

[14] W.W. Moses, *Current trends in scintillator detectors and materials*, Nucl. Instr. Meth. **A** 487 (2002) 123-128

[15] E.H. Darlington, *Backscattering of 10-100 keV electrons from thick targets*, J. Phys. **D**, Vol. 8, (1975) 85-93

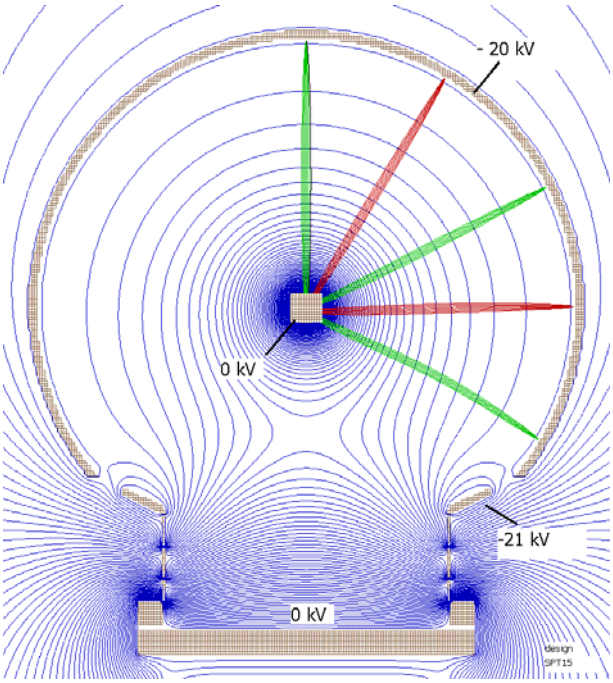

Fig. 1: Electrostatic configuration of the X-HPD. The simulation has been performed with the 3D tracking code SIMION 7.0. A number of electron trajectories at polar angles 0, 30, 60 and 90 degrees are indicated. For each emission point trajectories at angles up to ±30° relative to the surface normal are shown.

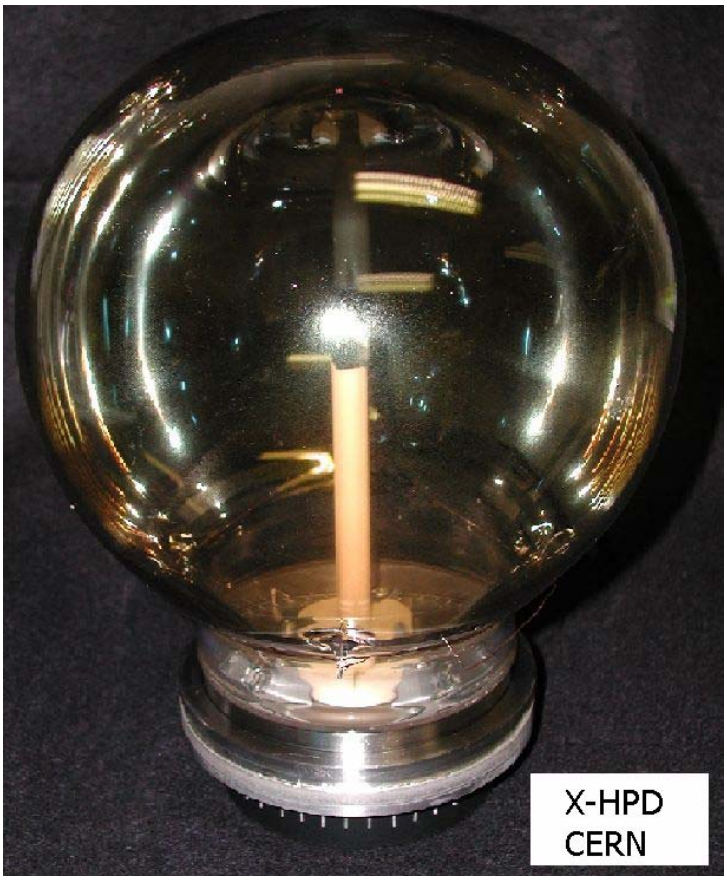

Fig. 2: Photograph of the X-HPD prototype with 208 mm diameter glass envelope.

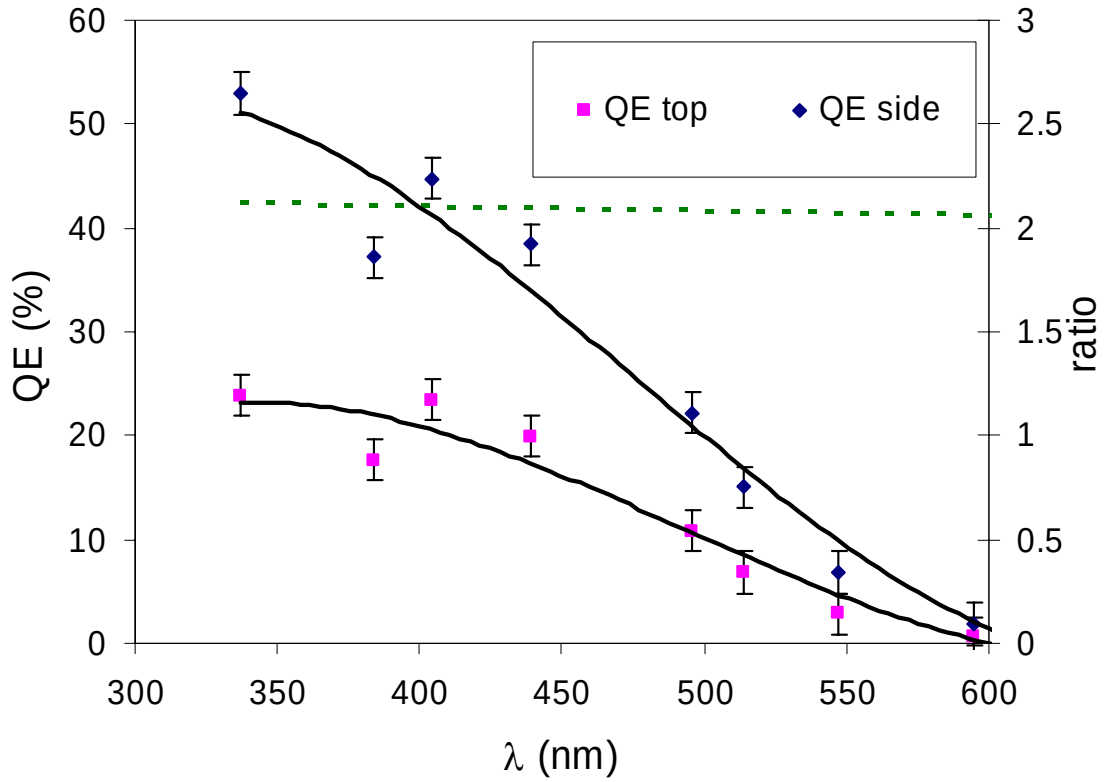

Fig. 3: Results of the quantum efficiency measurements with the standard set-up at Photonis.

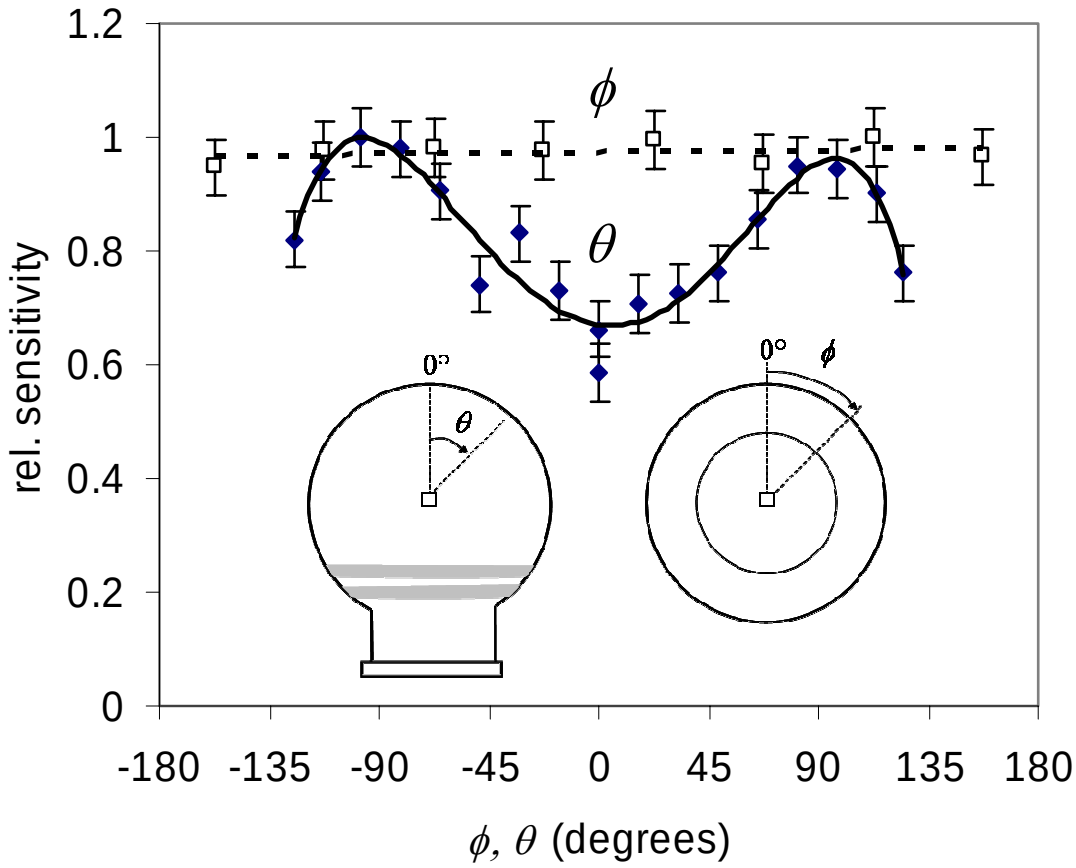

Fig. 4: Relative sensitivity measured with a blue LED (400 nm, ±15° emission angle). The anode was set to +300 V, the photocathode was at ground potential. The surface was scanned in polar (full symbols) and azimuthal (open symbols) direction (at $\theta = 90°$). The measured photocurrents were normalized to the highest value in the scan.

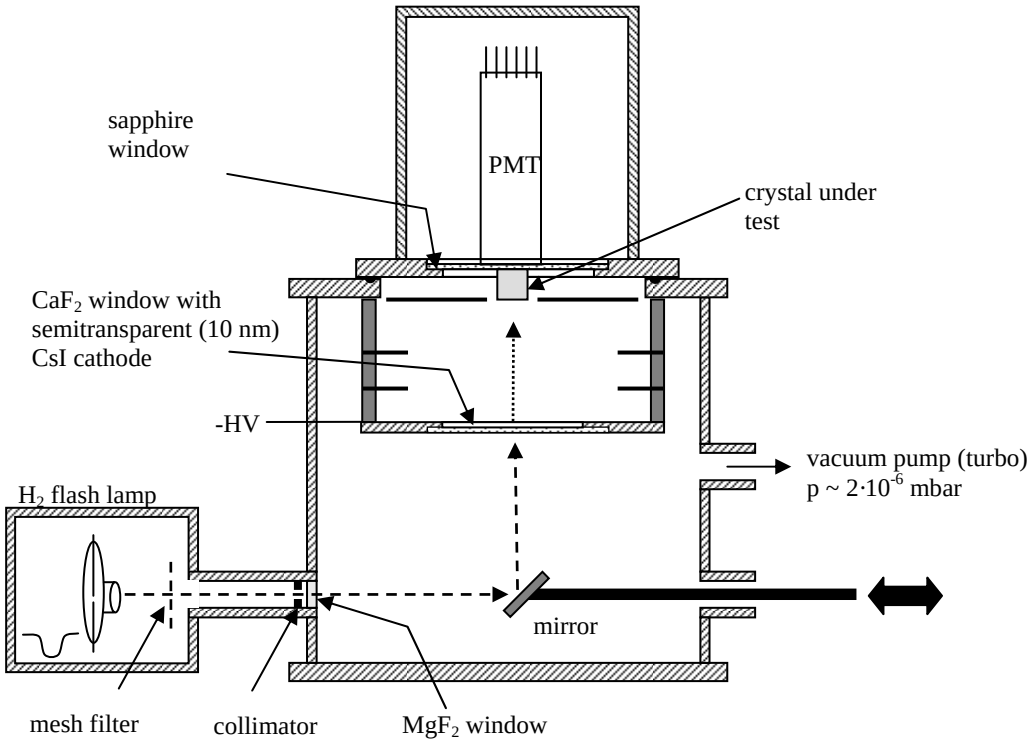

Fig. 5: Set-up for the test of scintillation crystals. UV light pulses from the D_2 flash lamp release photoelectrons from the CsI cathode which, after acceleration in an E-field bombard the scintillator crystal under test.

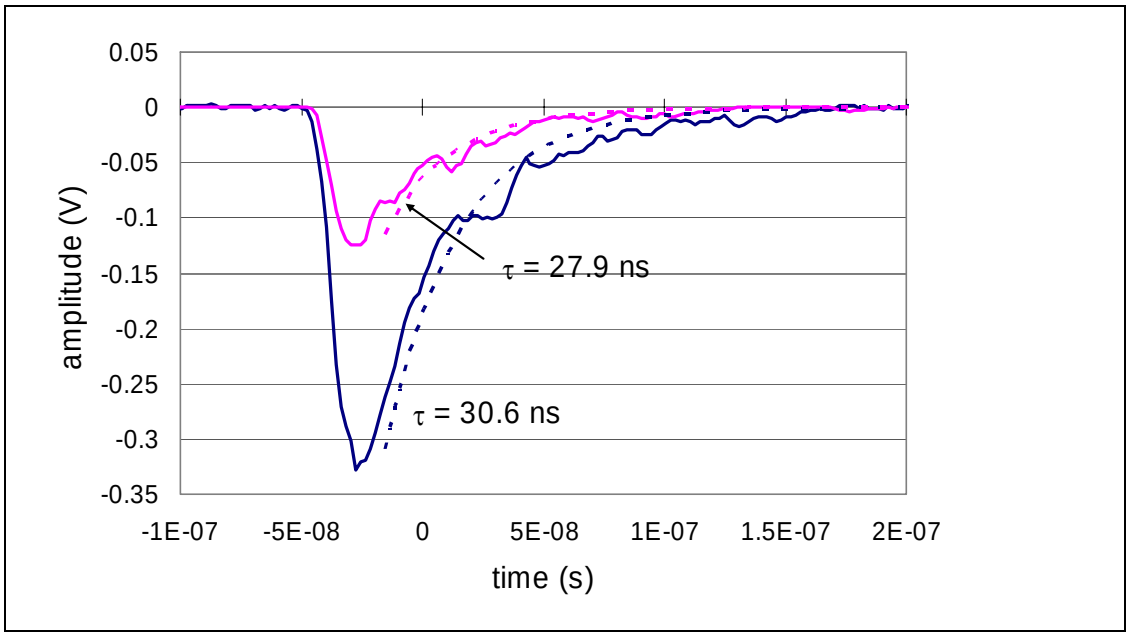

Fig. 6: Readout of the LSO crystal with PMT. The plot shows randomly selected typical waveforms recorded with the digital scope. The exponential decay of the scintillation light is clearly visible.

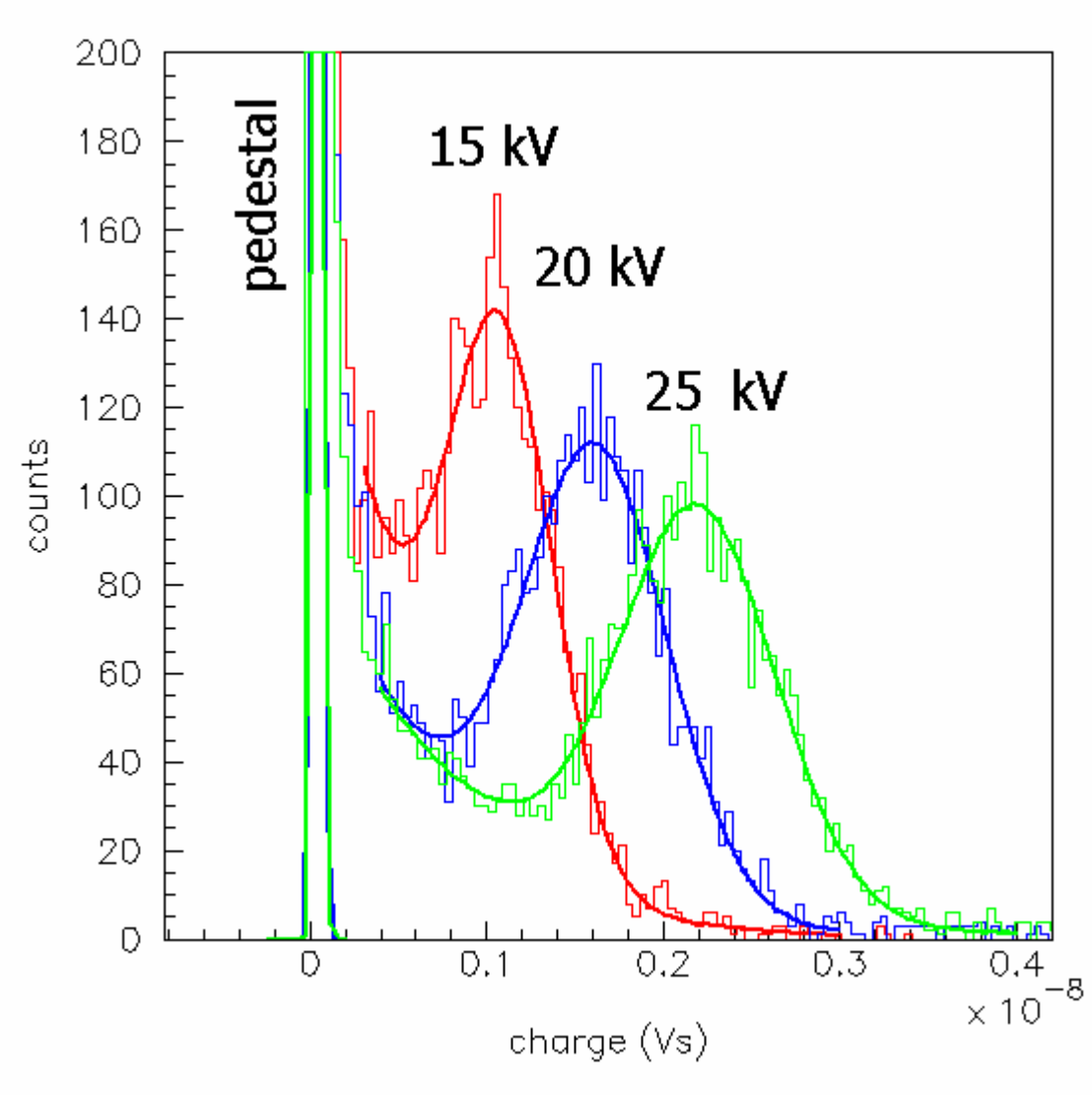

Fig. 7: LSO crystal read out with the PMT. Charge amplitude distributions for different voltage settings of the CsI cathode. The intensity of the flash tube was reduced to have practically only single photoelectrons emitted by the CsI cathode. The pedestal peaks are cut at 200 counts.

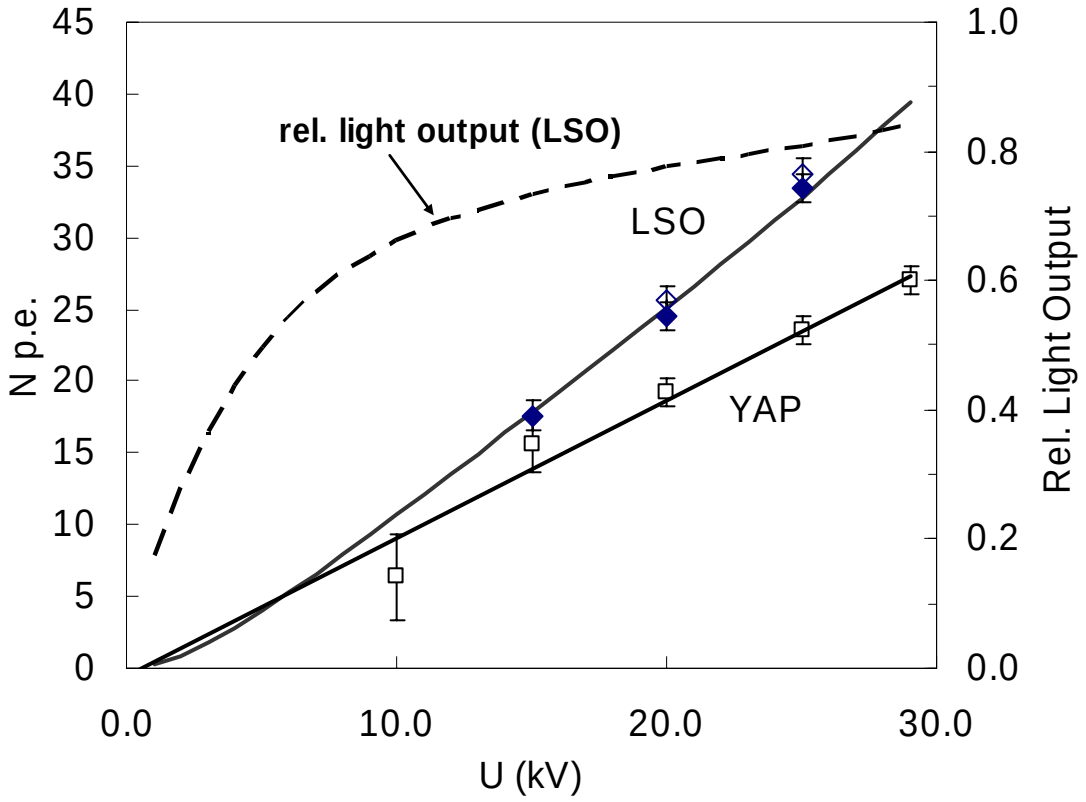

Fig. 8: LSO crystal with PMT readout. The plot shows the reconstructed number of photoelectrons as function of the applied voltage at the CsI cathode. Full and open symbols correspond to U_{PMT} = 1000 V and 900 V, respectively. The fits to the data are explained in the text. The relative light output of LSO [13][14] is shown as dashed line (secondary axis).

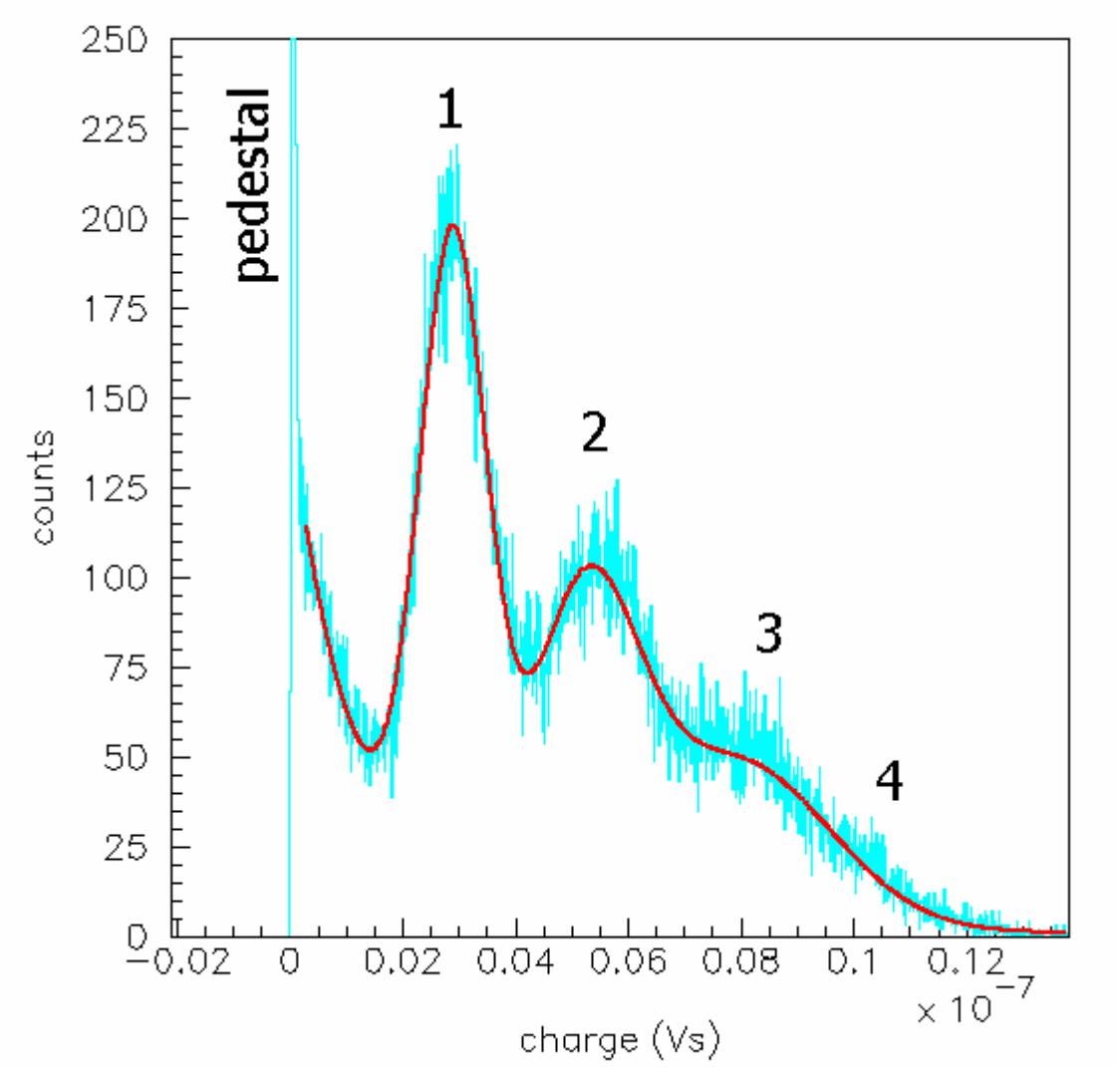

Fig. 9: LSO crystal read out with PMT. As previous figure, however the light intensity of the flash tube was increased. On average there is about 1 photoelectron. The pedestal peak is cut at 250 counts.